DOI: 10.1002/asia.201100028

Stereoaligned Epitaxial Growth of Single-Crystalline Platinum Nanowires by Chemical Vapor Transport

Youngdong Yoo,[a] Sol Han,[a] Minjung Kim,[b] Taejoon Kang,[a] Juneho In,[a] and Bongsoo Kim*[a]

Abstract: Epitaxial Pt nanowire (NW) arrays are synthesized for the first time by a chemical vapor transport method by using a metal halide as a precursor. Here we report that the epitaxial growth direction of NWs can be steered by seed crystal morphology. Octahedral seeds grow into inclined NWs possessing six growth directions, whereas half-octahedral seeds grow into vertical and horizontal NWs. Interfacial energies between the seed material and the substrate are critical in determining the morphology of seed crystals. We also demonstrate that non-SERS-active Pt NWs can show strong surface-enhanced Raman scattering (SERS) spectra by placing them on Ag films. The active SERS observation would help to elucidate platinum-catalyzed chemical reactions.

Keywords: epitaxial growth · gold · nanowires · platinum · Raman spectroscopy

Introduction

Platinum is employed as one of the major catalysts in industrial reactions, such as catalytic conversion of automobile pollutant gases, oxygen reduction reaction in fuel cells, and hydrogenation reactions.[1–3] As catalytic activity and selectivity are strongly affected by the surface atomic structure of the nanomaterial,[4] Pt nanowire (NW) arrays with well-defined facets can be employed for detailed investigation of surface-dependent catalytic properties. Freestanding Pt NWs epitaxially grown on a substrate would be optimum for this purpose.

Recently, we reported that epitaxial Au, Pd, and AuPd NWs can grow through a physical vapor transport method by using a metal slug or powder as the source.[5,6] This method, however, could not be employed for the synthesis of Pt NWs because of a low vapor pressure of Pt. Although various methods for growth of Pt NWs have been developed,[7–13] freestanding and single-crystalline Pt NWs without defects that have high aspect ratios and well-defined facets have not been reported yet. We have synthesized epitaxially grown and single-crystalline Pt NWs for the first time by employing a metal halide as a precursor. This synthetic method is based on simple modification of the van-Arkel method used for the separation or purification of metals through vapor transport.[14] Because metal halides have a relatively high vapor pressure at a low temperature, this method could be employed more generally to noncatalytic growth of NWs composed of other metals possessing low vapor pressures.

We have already reported that Au NWs grow vertically or horizontally from half-octahedral seeds, depending on the magnitude of atom flux.[5] In this study, we observed that NW growth can also be initiated from octahedral seeds, resulting in six inclined NW growth directions. So far epitaxial growth directions of NWs have been controlled by changing the crystal orientation of the substrate surface or by changing the atom flux. Here we suggest epitaxial growth directions of NWs can be steered by seed crystal morphology.

Vapor-phase NW growth initiated from seeds reported in this paper is distinctly different from conventional solution-phase seeded NW growth. While seed crystals in solution-phase NW growth are added independently,[15,16] seed crystals in our methods are formed spontaneously in the initial stage of supplying atomic building blocks and then aniso-

[a] Y. Yoo, S. Han, T. Kang, J. In, Prof. B. Kim
Department of Chemistry
KAIST
Daejeon 305-701 (Korea)
Fax: (+82) 42-350-2810
E-mail: bongsoo@kaist.ac.kr

[b] M. Kim
Graduate School of Nanoscience and Technology
KAIST
Daejeon 305-701 (Korea)

Supporting information for this article is available on the WWW under http://dx.doi.org/10.1002/asia.201100028.

tropic nanostructures grow from these seed crystals.[5] Thus, seed formation in our methods should be understood as an initial step in the total growth process.

After the $PtCl_2$ vapor collides with the substrate, Pt atoms condense on a sapphire substrate to form half-octahedral seeds and octahedral seeds. The seed formation process is strongly affected by the interfacial energy between the seed material and the substrate. As these seeds are epitaxially formed, depending on the crystallographic relationship with the substrate, the NWs grown from these seeds also have specific growth directions and thus epitaxial growth of NWs can be accomplished.

We have also investigated surface enhanced Raman scattering (SERS) enhancement on Pt NWs. By fabricating a novel SERS platform composed of a well-faceted Pt NW on an Ag film, we obtained high-quality SERS spectra of the molecular species adsorbed on non-SERS-active Pt NW surfaces. Whereas Ag and Au are widely utilized as effective materials for SERS, Pt has been commonly known as a non-SERS-active material.[17,18] SERS enhancement on Pt surfaces can be quite valuable to in-depth studies of platinum-catalyzed chemical reactions.[19–21]

Results and Discussion

Growth of Pt NWs from Half-Octahedral Seeds: Vertical and Horizontal Growth

When $PtCl_2$ precursor temperature is maintained at 400 °C, vertically grown Pt NWs are synthesized on a c-cut sapphire substrate (Figure 1 a). Lengths of NWs are 5–10 μm and diameters of NWs are 70–150 nm. The morphology of the NWs is similar to those of Au, Pd, and AuPd NWs previously reported.[5] These vertical NWs are aligned in three orientations at 120° to one another (Figure 1 b), and the epitaxial relationship between a vertical NW and c-cut sapphire is (110) Pt//(0001) sapphire. The geometry and orientation of half-octahedral nanocrystals are the same as those of vertical NWs (compare the insets in Figure 1 a and c); this suggests that the vertical Pt NWs grow from the half-octahedral nanocrystals (seeds). TEM data and the XRD pattern confirm that as-synthesized NWs are Pt with a face-centered cubic structure and have a single crystalline nature and a [110] growth direction (see Figures S1 and S2 in the Supporting Information).

We reported that the growth direction (vertical or horizontal) of Au, Pd, and AuPd NWs can be selected by changing the deposition flux.[5] These NWs grow vertically or horizontally from the same half-octahedral seeds, depending on experimental conditions. We can control the growth direction of Pt NWs through the same methods. When we increase Pt deposition flux by raising the precursor temperature to 800 °C, horizontal NWs instead of vertical NWs grow on a c-cut sapphire substrate (Figure 1 d). A magnified SEM image shows that the NW is well-faceted and has a shape of an elongated half-octahedron (the inset in Figure 1 d).

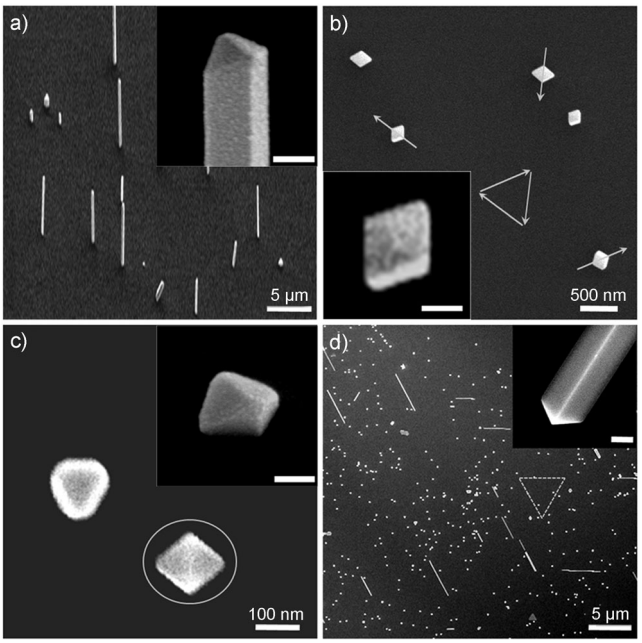

Figure 1. Pt NWs grown vertically and horizontally on a c-cut sapphire substrate. a) 45° tilted SEM image of the vertical Pt NWs. The inset is a magnified SEM image showing the tip of the NW (scale bar: 100 nm). b) Top-view SEM image of the vertical Pt NWs. The inset is a magnified top-view SEM image of the vertical NW (scale bar: 100 nm). c) Top-view SEM image of a half-octahedral Pt seed (gray circle) and an octahedral Pt seed. The inset is a 45° tilted SEM image of a half-octahedral seed (scale bar: 100 nm). d) Top-view SEM image of the horizontal Pt NWs. The inset is a magnified SEM image showing the tip of the NW (scale bar: 100 nm).

Growth of Au and Pt NWs from Octahedral Seeds: Inclined Growth

Although both half-octahedral seeds and octahedral seeds are formed on the substrate, it has been observed that vertical and horizontal growth are initiated from only half-octahedral seeds. We have observed that epitaxial NW growth can also be initiated from the octahedral seeds under appropriate experimental conditions. Here we report the inclined growth of Au and Pt NWs initiated from octahedral seeds. Figure 2 a shows the inclined Au NWs synthesized at the end edge part of the substrate at a source temperature of 1100 °C. The top-view image in Figure 2b indicates three inclined growth directions (actually six directions, as discussed below) with in-plane components at 120° to one another. The inset in Figure 2 b indicates that the inclined NW is well-faceted and has an elongated octahedral shape. Inclined NWs grow along $<110>$ directions of an octahedral seed and are enclosed by the most stable {111} top and side facets. The angle between the NW grown along $<110>$ directions and the substrate is calculated to be 54.74° (Figure 2 c).

Figure 2 d shows octahedral Au nanocrystals found on the substrate. The octahedral seed can have one of two orientations, labeled X and Y in Figure 2 d, as the triangular base can sit on the c-cut sapphire substrate in two equivalent ori-

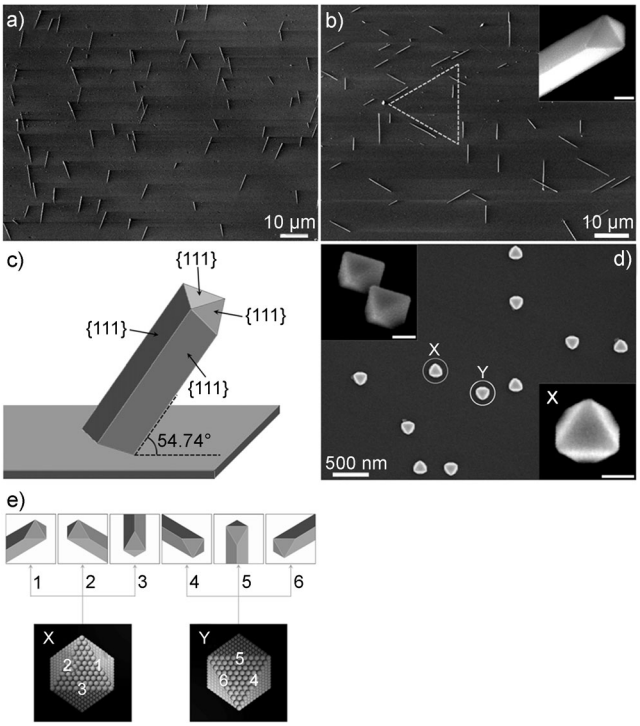

Figure 2. Au NWs grown in a tilted direction on a c-cut sapphire substrate. a) 45° tilted SEM image of inclined Au NWs. b) Top-view SEM image of inclined Au NWs. The inset is a magnified top-view SEM image of an inclined Au NW (scale bar: 100 nm). c) Structural model of the inclined NW grown on the substrate. d) Top-view SEM image of octahedral Au seeds. The upper-left inset shows a 45° tilted and magnified SEM image and the lower-right inset shows a top-view magnified SEM image of an octahedral seed (scale bars: 100 nm). The octahedral seed can have two orientations labeled X and Y. e) Schematic illustration of the growth pathways from octahedral seeds to inclined Au NWs. Numbered six top-view images of inclined NWs represent the growth along the six possible <110> directions that are normal to six (110) edges (correspondingly numbered) of the top face of the seed for X and Y orientations.

entations (see Figure S3 in the Supporting Information). Considering the correlations of the geometry and orientations of the octahedral nanocrystals with those of the inclined NWs, we can visualize that the inclined NWs grow from octahedral seeds along three possible <110> directions normal to three {110} edges of the top face of the seed. Thus we have a total of six inclined growth directions starting from the two seed orientations (X and Y), as illustrated by the six top-view diagrams in Figure 2e. These appear as three growth directions in the top-view image of Figure 2b.

Similar inclined growth of Pt NWs is also observed at the end edge part of the substrate (Figure 3a). The $PtCl_2$ precursor temperature was 400 °C. Octahedral Pt nanocrystals are observed on the same substrate in two orientations at 180° to one another (Figure 3b). These nanocrystals are considered to be seeds of the inclined NWs. Figure 3c shows a top-view SEM image of an inclined NW and an octahedral seed.

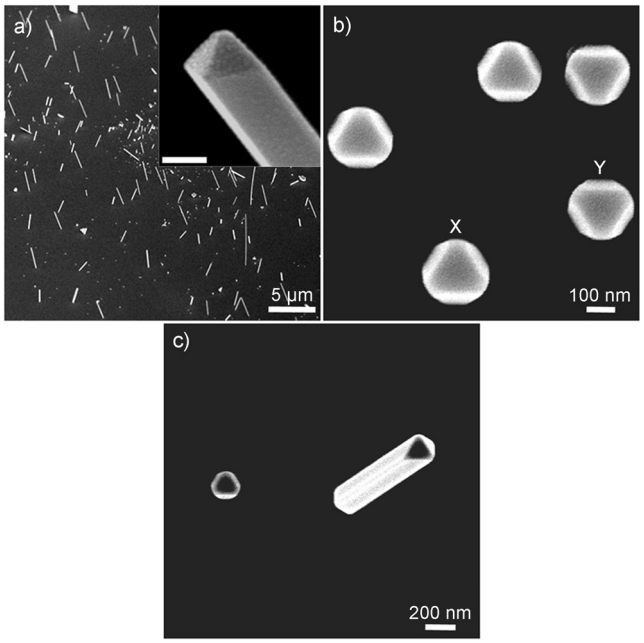

Figure 3. Pt NWs grown in a tilted direction on a c-cut sapphire substrate. a) 45° tilted SEM image of the Pt NWs. The inset is a magnified SEM image showing the tip of the NW (scale bar: 100 nm). b) Top-view SEM image of the octahedral Pt seeds. The octahedral seed can have two orientations labeled X and Y. c) Top-view SEM image of an inclined Pt NW and its octahedral seed.

Epitaxial Crystalization of Octahedral Seeds and Half-Octahedral Seeds on Substrates

The Pt atoms arriving on the substrate will diffuse and nucleate to form small nanocrystals. The shape of the nanocrystals is determined by the surface energies of the nanocrystal facets and the interface energy between the nanocrystal and the substrate. When Pt nanocrystals have a (111) interface with the substrate, octahedral seeds can be formed. When Pt nanocrystals have a (110) interface with the substrate, half-octahedral seeds can be obtained.

Figure 4a is a structural model (top view) of an octahedral seed, all facets of which are made up of {111} facets. Figure 4c illustrates atomic planes at the epitaxial interface between the octahedral Pt seed and c-cut sapphire. The lattice mismatch between a {111} bottom plane of Pt and c-cut sapphire is 1.16% along the Pt <110> direction and 0.84% along the Pt <112> direction. Figure 4b is a structural model (45° tilted view) of a half-octahedral seed. The half-octahedral seed can be obtained by bisecting the octahedral seed, and possesses {110} bottom plane. Figure 4d illustrates atomic planes at the epitaxial interface between the half-octahedral Pt seed and c-cut sapphire. The lattice mismatch between {110} Pt and c-cut sapphire is 5.02% along the Pt <100> direction and 52.52% along the Pt <110> direction (the lattice mismatch is 2.70% along the Pt <110> direction when we consider a larger domain, in which five layers of Pt are matched with three layers of sapphire). Seed formation is strongly affected by the interfacial energy correlated with the lattice mismatch between the seed material

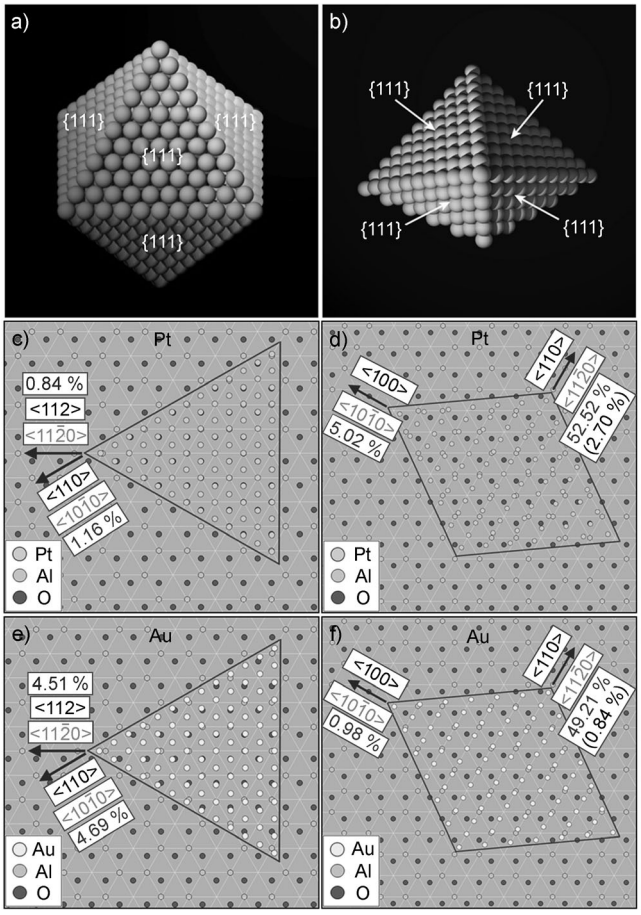

Figure 4. a) Structural model (top-view) of an octahedral seed. b) Structural model (45° tilted view) of a half-octahedral seed. c) Schematic of atomic planes at the epitaxial interface between the octahedral Pt seed and c-cut sapphire. d) Schematic of atomic planes at the epitaxial interface between the half-octahedral Pt seed and c-cut sapphire. e) Schematic of atomic planes at the epitaxial interface between the octahedral Au seed and c-cut sapphire. f) Schematic of atomic planes at the epitaxial interface between the half-octahedral Au seed and c-cut sapphire.

and the substrate.[22] Thus, the number of octahedral Pt seeds formed on the c-sapphire substrate is 10–20 times larger than that of half-octahedral Pt seeds because of the better lattice match between the octahedral seed and c-cut sapphire.

In the case of Au, the lattice mismatch between the octahedral seed and c-cut sapphire is about 4.6% (Figure 4e). The lattice mismatch between the half-octahedral Au seed and c-cut sapphire is 0.98% along the Au $<100>$ direction and 49.21% along the Au $<110>$ direction (the lattice mismatch is 0.84% along the Au $<110>$ direction when we consider a larger domain, in which five layers of Au are matched with three layers of sapphire; Figure 4f). The number of octahedral Au seeds formed on the c-sapphire substrate is approximately 2–3 times larger than that of half-octahedral Au seeds.

Formation of half-octahedral Pt seeds is more difficult than that of half-octahedral Au seeds because of worse lattice mismatch on the c-cut sapphire substrate (compare Figure 4d with f). On the other hand, formation of octahedral Pt seeds is easier than that of octahedral Au seeds, because of better lattice mismatch (compare Figure 4c with e).

Growth Mechanism of Noble Metal NWs from Octahedral and Half Octahedral Seeds

As the density of half-octahedral Pt seeds is lower than that of half-octahedral Au seeds, the densities of vertical and horizontal Pt NWs grown from half-octahedral seeds are lower than those of vertical and horizontal Au NWs, respectively. Because the density of octahedral Pt seeds is higher than that of octahedral Au seeds, the density of inclined Pt NWs grown from octahedral seeds is higher than that of inclined Au NWs.

Why is vertical growth from half-octahedral seeds mostly observed in spite of dominant formation of octahedral seeds at the central part on the substrate? NW growth from the seeds is strongly affected by local flow conditions. At the central part on the substrate, the material flux direction would be nearly perpendicular to the substrate, whereas at the edge of the substrate turbulent flow might occur due to the geometrical shape. When the material flux direction is perpendicular to the substrate, vertical growth from the half-octahedral seed would be more favored than inclined growth from the octahedral seed because of more advantageous solid angle of collision for NW growth. Inclined growth from octahedral seeds, however, is often observed near the end edge part of the substrate.

NW growth from seeds can occur along $<110>$ directions of half-octahedral and octahedral seeds, because the NWs can be enclosed by the energetically most stable {111} facets in this case. Thus, half-octahedral seeds with {110} bottom facets can grow vertically or horizontally and octahedral seeds with {111} bottom facets can grow along the three inclined directions (54.74° with respect to the substrate). Because the octahedral seeds have two orientations at angles 180° to one another, a total of six inclined growth directions are possible.

SERS Enhancement of Pt NWs

The SERS enhancement is strongly dependent on the detailed morphology of metal nanostructures. Fabricating well-defined and reproducible SERS platforms is greatly desirable for SERS applications. Pt NWs possessing a single-crystalline nature and atomically smooth surfaces can be utilized for fabricating a well-defined and reproducible SERS platform.

To obtain SERS spectra of the molecular species adsorbed on the non-SERS-active Pt NW, we fabricated a novel SERS platform composed of a single Pt NW on an Ag film. After incubation of Pt NWs in a benzenethiol (BT) or brilliant cresyl blue (BCB) solution, the Pt NWs are cast on a smooth Ag film (see the inset in Figure 5a). Figure 5a,b shows polarization-dependant SERS spectra of BT and BCB adsorbed on a single Pt NW on a Ag film. Strong enhance-

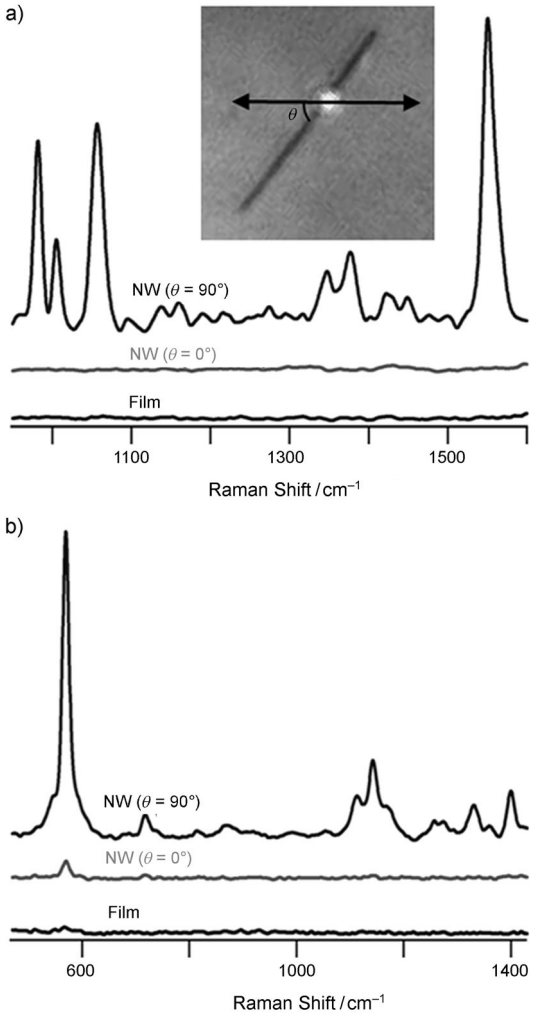

Figure 5. SERS spectra of a) BT and b) BCB adsorbed on a single Pt NW on a Ag film when $\theta = 0$ and $\theta = 90°$; θ is the angle between the NW axis and the polarization of light. Inset is optical microscope image of a single Pt NW on an Ag film.

ment of the SERS signal is observed when the polarization direction is perpendicular to the NW axis ($\theta = 90°$), but the SERS signal almost disappears when the polarization direction is parallel to the NW axis ($\theta = 0°$). A strongly enhanced electric field is induced at the gap between the NW and the film by light with perpendicular polarization, but this enhancement is not induced by light with parallel polarization.[23–25]

Conclusions

By employing a chemical vapor transport method by using a metal halide as a precursor, we have epitaxially grown stereoaligned Pt NW arrays on a c-cut sapphire substrate. Vertical and horizontal NWs grow from half-octahedral seeds and inclined NWs from octahedral seeds. The epitaxial growth direction of NWs is determined by the morphology of seed crystals. In addition, high-quality SERS spectra of BT and BCB adsorbed on non-SERS-active Pt NW surfaces are obtained by fabricating a novel SERS platform composed of a Pt NW on an Ag film.

Experimental Section

Synthesis and Characterization of Pt NWs

Pt NWs are synthesized in a horizontal two-zone furnace with a 1 inch diameter inner quartz tube via a chemical vapor transport method by using $PtCl_2$ powder as a precursor without using any catalysts (see Figure S4 in the Supporting Information). The $PtCl_2$ precursor is evaporated at 400–800 °C and transported to a sapphire substrate at the high-temperature (1000 °C) region by carrier gas (Ar), at which Pt is deposited after the dissociation of $PtCl_2$ on a hot substrate ($PtCl_2 \rightarrow Pt + Cl_2$). Ar gas flowed at a rate of 300 sccm with the chamber pressure maintained at 760 Torr. The reaction time was 30–60 min. Field emission SEM images were taken on a Phillips XL30S. Samples were coated with gold to avoid charging effect during the SEM observation. TEM images, HRTEM images, and selected area electron diffraction (SAED) patterns were taken on a TECNAI F30 TEM operated at 300 kV.

Raman Spectroscopy

Smooth Ag films were fabricated on Si substrates by electron beam-assisted deposition of 10 nm of Cr followed by 300 nm of Ag. For BT experiments, Pt NWs were incubated in a 1 mM BT solution in ethanol for 24 h. For BCB experiments, Pt NWs were incubated in a 1 μM BCB solution in ethanol for 30 min. A drop of an incubated Pt NW solution was cast on an Ag film. The SERS platforms were rinsed with an excess of ethanol and purged with nitrogen to remove the excess solvent. SERS spectra were obtained by using a home-built micro-Raman system. The 633 nm light of a He-Ne laser (Melles Griot) was utilized as an excitation source and the laser light (~500 nm diameter) was focused on a sample through a ×100 objective (Mitutoyo). The SERS signal was collected with the same objective. The polarization direction of laser light was controlled by rotating a half-wave plate.

Acknowledgements

This research was supported by KOSEF through NRL (20100018868), SRC (2011-0001335), and "Center for Nanostructured Material Technology" under the "21st Century Frontier R&D Programs" (2011K000210) of the MEST, Korea.

[1] A. Roucoux, J. Schulz, H. Patin, *Chem. Rev.* **2002**, *102*, 3757–3778.
[2] B. Lim, M. Jiang, P. H. C. Camargo, E. C. Cho, J. Tao, X. Lu, Y. Zhu, Y. Xia, *Science* **2009**, *324*, 1302–1305.
[3] H. Song, R. M. Rioux, J. D. Hoefelmeyer, R. Komor, K. Niesz, M. Grass, P. Yang, G. A. Somorjai, *J. Am. Chem. Soc.* **2006**, *128*, 3027–3037.
[4] V. Komanicky, H. Iddir, K.-C. Chang, A. Menzel, G. Karapetrov, D. Hennessy, P. Zapol, H. You, *J. Am. Chem. Soc.* **2009**, *131*, 5732–5733.
[5] Y. Yoo, K. Seo, S. Han, K. S. K. Varadwaj, H. Y. Kim, J. H. Ryu, H. M. Lee, J. P. Ahn, H. Ihee, B. Kim, *Nano Lett.* **2010**, *10*, 432–438.
[6] Y. Yoo, I. Yoon, H. Lee, J. Ahn, J.-P. Ahn, B. Kim, *ACS Nano* **2010**, *4*, 2919–2927.
[7] E. U. Donev, J. T. Hastings, *Nano Lett.* **2009**, *9*, 2715–2718.
[8] J. Shui, J. C. M. Li, *Nano Lett.* **2009**, *9*, 1307–1314.
[9] E. Formo, E. Lee, D. Campbell, Y. Xia, *Nano Lett.* **2008**, *8*, 668–672.
[10] E. P. Lee, Z. Peng, D. M. Cate, H. Yang, C. T. Campbell, Y. Xia, *J. Am. Chem. Soc.* **2007**, *129*, 10634–10635.
[11] S. Sun, F. Jaouen, J.-P. Dodelet, *Adv. Mater.* **2008**, *20*, 3900–3904.

[12] X. Teng, W.-Q. Han, W. Ku, M. Hücker, *Angew. Chem.* **2008**, *120*, 2085–2088; *Angew. Chem. Int. Ed.* **2008**, *47*, 2055–2058.
[13] J. Chen, Y. Xiong, Y. Yin, Y. Xia, *Small* **2006**, *2*, 1340–1343.
[14] A. E. van Arkel, J. H. de Boer, *Z. Anorg. Allg. Chem.* **1925**, *148*, 345- 350.
[15] Y. Sun, B. Mayers, T. Herricks, Y. Xia, *Nano Lett.* **2003**, *3*, 955–960.
[16] Y. Sun, Y. Yin, B. T. Mayers, T. Herricks, Y. Xia, *Chem. Mater.* **2002**, *14*, 4736–4745.
[17] M. E. Abdelsalam, S. Mahajan, P. N. Bartlett, J. J. Baumberg, A. E. Russell, *J. Am. Chem. Soc.* **2007**, *129*, 7399–7406.
[18] K. Ikeda, J. Sato, N. Fujimoto, N. Hayazawa, S. Kawata, K. Uosaki, *J. Phys. Chem. C* **2009**, *113*, 11816–11821.
[19] K. N. Heck, B. G. Janesko, G. E. Scuseria, N. J. Halas, M. S. Wong, *J. Am. Chem. Soc.* **2008**, *130*, 16592–16600.
[20] H.-F. Yang, J. Feng, Y.-L. Liu, Y. Yang, Z.-R. Zhang, G.-L. Shen, R.-Q. Yu, *J. Phys. Chem. B* **2004**, *108*, 17412–17417.
[21] C. Shi, W. Zhang, R. L. Birke, J. R. Lombardi, *J. Phys. Chem.* **1990**, *94*, 4766–4769.
[22] F. Silly, M. R. Castell, *Phys. Rev. Lett.* **2005**, *94*, 046103.
[23] S. J. Lee, J. M. Baik, M. Moskovits, *Nano Lett.* **2008**, *8*, 3244–3247.
[24] H. Wei, F. Hao, Y. Huang, W. Wang, P. Nordlander, H. Xu, *Nano Lett.* **2008**, *8*, 2497–2502.
[25] I. Yoon, T. Kang, W. Choi, J. Kim, Y. Yoo, S.-W. Joo, Q-H. Park, H. Ihee, B. Kim, *J. Am. Chem. Soc.* **2009**, *131*, 758–762.

Received: January 15, 2011
Published online: May 18, 2011

